

SPARK AND VOLUME IGNITION OF DT AND D₂ MICROSPHERES

M.M. BASKO

Institute of Theoretical and Experimental Physics,
Moscow,
Union of Soviet Socialist Republics

ABSTRACT. Admissible values of the temperature T_s and the confinement parameter $H_s = \rho_s R_s$ of a hot thermonuclear spark in DT and D₂ fuels have been investigated. It is shown that it is not possible to achieve spark ignition of pure deuterium targets. Numerical simulations of precompressed DT and D₂ microspheres (bare or tamped with a gold shell) have been performed and the values of the spark factor f_s (ratio of thermonuclear energy gains that can be achieved in optimal core ignited and volume ignited targets) have been calculated. For a few milligrams of equimolar DT mixture the spark factor is shown to be 1.8–1.9, while for 10 mg D₂ microspheres it is below 1.2.

1. INTRODUCTION

When designing thermonuclear targets of high energy gain for inertial confinement fusion (ICF), special attention is paid to the concept of central spark ignition [1–8]. According to this concept, a hot central spot (a thermonuclear spark) is formed in the imploding fuel microsphere, which then ignites and initiates a thermonuclear burn wave that propagates to the outer cold fuel layers.

The concept of a thermonuclear spark has been put forward as an alternative to volume ignition, by which the more or less homogeneously compressed and heated fuel is ignited simultaneously over the entire mass. Various calculations of DT targets driven by laser and ion beams have shown that, depending on the target design and the driver parameters, either kind of ignition can occur. A priori, it is quite clear that, regarding the energy gain, spark ignition is more advantageous because only a small portion of the fuel has to be heated to relatively high ignition temperatures. Some authors [5, 9] even argue that with volume ignition it is not possible to reach the target gains of $G > 20$ –40 required for a thermonuclear power station. However, other researchers [10, 11] have calculated that high enough gains for uniformly ignited targets can be achieved.

To resolve this controversy, the following question has to be answered: quantitatively, how much better is the best spark ignition configuration compared to the best volume ignition configuration with the same fuel mass? In this paper we present an answer to this question for initially compressed DT and D₂ microspheres for which it is assumed that the step-like initial temperature and density profiles have a uniform pressure distribution. The advantage of spark ignition is

characterized by the value of the spark factor f_s , defined as the ratio of the corresponding optimal gain values. The values of f_s have been calculated for (1) a bare DT sphere of mass $M_f = 1$ mg, (2) a DT sphere ($M_f = 1$ mg) tamped with a compressed gold shell of mass $M_t = 10 M_f = 10$ mg, and (3) a 10 mg D₂ sphere with a 100 mg gold tamper. The resulting values of f_s for 1 mg of equimolar DT mixture have turned out to be 1.8–1.9, i.e. the performance of spark ignition is improved by *no more than a factor of two* compared with that of optimal, uniformly ignited targets. For pure deuterium targets with $M_f = 10$ mg, $f_s < 1.2$, and spark ignition in the proper sense does not occur at all.

2. ADMISSIBLE VALUES OF SPARK PARAMETERS

We assume that the initial fuel configuration is a compressed sphere of uniform pressure, consisting of a hot central spark (temperature T_s , density ρ_s , radius R_s) and a cold outer fuel layer (temperature T_c , density ρ_c , radius R_f). As pointed out by Meyer-ter-Vehn [6], the spark profile of uniform pressure is in better agreement with 1-D hydrodynamics target simulations than the isochoric distribution adopted in earlier publications [1–3, 12]. A posteriori, one can easily verify that equal temperatures can be postulated for ions and electrons in the spark region. Then, to characterize the physical conditions in the spark, one needs only two parameters — the plasma temperature T_s and the confinement parameter $H_s = \rho_s R_s$.

Here, we consider the constraints on the possible values of these parameters imposed by the following two conditions of spark ignition: (i) a spark with given

values of T_s and H_s can be formed in the process of hydrodynamic implosion, and (ii) a spark with given values of T_s and H_s can ignite, i.e. the thermonuclear self-heating of the spark region exceeds the energy losses due to cooling.

Cooling of the spark is dominated by the bremsstrahlung and the electron heat conduction. The rate of bremsstrahlung energy losses from a hydrogen isotope plasma is given by

$$q_{ff} [\text{erg} \cdot \text{s}^{-1} \cdot \text{electron}^{-1}] = 5.36 \times 10^{-24} n_e T_s^{1/2} \quad (1)$$

Here, and henceforth, T_s is in units of keV (note that in all cases of interest the spark region is transparent to its own radiation). The cooling rate due to electron thermal conductivity can be evaluated as

$$q_{ec} [\text{erg} \cdot \text{s}^{-1} \cdot \text{electron}^{-1}] = 3\kappa_{ec} \frac{kT_s}{n_e R_s^2} \quad (2)$$

where κ_{ec} is the electron thermal conductivity coefficient, $k = 1.6 \times 10^{-9}$ erg/keV. A spark with the parameters T_s , R_s , ρ_s can be created by means of the hydrodynamic implosion only if the cooling time-scale

$$t_c = \frac{3kT_s}{q_{ff} + q_{ec}} \equiv \frac{1}{t_{ff}^{-1} + t_{ec}^{-1}} \quad (3)$$

is of the same order of magnitude or greater than the time

$$t_s [\text{s}] = \frac{R_s}{c_s} = 1.76 \times 10^{-8} \bar{A}^{1/2} R_s T_s^{-1/2} \quad (4)$$

of sound propagation across the spark region in the final stage of its formation (for example behind the reflected shock wave if the spark results from a strong shock converging to the centre); \bar{A} is the mean atomic weight of the fuel that consists of deuterium and tritium at some initially fixed proportion. With Eqs (1)–(4), the condition $t_c > t_s$ of spark formation takes the form

$$12 \bar{A}^{-1/2} \frac{H_s}{T_s} + 1.8 \times 10^{-3} \bar{A}^{3/2} \frac{T_s^2}{H_s \ln \Lambda} \leq 1 \quad (5)$$

Here, the Spitzer value of κ_{ec} [13] has been used; the Coulomb logarithm $\ln \Lambda$ is given by

$$\ln \Lambda = \ln \left[60 T_s \left(\frac{\bar{A}}{\rho_s} \right)^{1/2} \right] \quad (6)$$

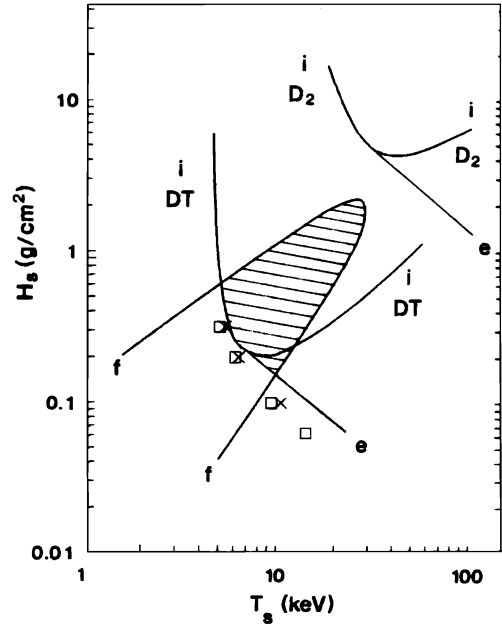


FIG. 1. Admissible values of the thermonuclear spark parameters. The region inside curve *f* is defined by the criterion of spark formation. Sparks with parameters above the curves *i*–*e* satisfy the ignition criterion in DT and D_2 fuels. The hatched region satisfies both criteria in equimolar DT. The threshold ignition parameters obtained for bare and tamped DT microspheres in hydrodynamic simulations are marked by crosses and open squares, respectively.

To the extent that the weak dependence of $\ln \Lambda$ on ρ_s can be neglected, inequality (5) defines a universal relationship between the admissible values of the spark parameters T_s and H_s , in the sense that ρ_s and R_s enter this relationship not separately but in combination, $H_s = \rho_s R_s$. In Fig. 1, the region of the T_s , H_s values allowed by formation criterion (5) lies inside curve *f* plotted for $\bar{A} = 2.5$; the Coulomb logarithm $\ln \Lambda$ was calculated for $\rho_s = 30$ g/cm³.

According to Eq. (5), the maximum temperature that can be reached in the spark is about 30 keV. Too large sparks, with $H_s > 0.08 \bar{A}^{1/2} T_s$, cannot form because of the bremsstrahlung energy losses ($t_{ff} < t_s$), while the formation of too small sparks, with $H_s < 1.8 \times 10^{-3} \bar{A}^{3/2} T_s^2 / \ln \Lambda$, is inhibited by the electron thermal conductivity ($t_{ec} < t_s$). Note that when we turn from equimolar DT to pure D_2 , the curve *f* in Fig. 1 undergoes only a minor deformation (the reduction of \bar{A} in the second term of Eq. (5) is more than compensated by higher typical values of ρ_s in the Coulomb logarithm), which we ignore below.

The spark ignites only if the thermonuclear heating rate

$$q_{\text{in}} = \sum_{ij} \langle \sigma v \rangle_{ij} \left(\frac{n_i n_j}{n_c} \right) \left(\sum_k Q_{ijk} f_{ijk} \right) \quad (7)$$

exceeds the cooling energy losses $q_{\text{ff}} + q_{\text{ec}}$ over the region $0 \leq r \leq R_s$. In Eq. (7), Q_{ijk} is the energy of the fast particle k born in the fusion reaction $i + j$, and f_{ijk} is the fraction of energy that the particle ijk deposits in the sphere of radius R_s . For charged fusion products, the deposition fraction f_{ijk} can be approximated by

$$f_{ijk} = \frac{H_s}{H_s + \frac{2}{3} H_{ijk}} \quad (8)$$

where H_{ijk} is the path length (in g/cm^2) of the product species ijk in a plasma with a temperature T_s and a density ρ_s . Equation (8) has correct asymptotics in both limits $H_s \ll H_{ijk}$ and $H_s \gg H_{ijk}$ [14], while in the intermediate region, $H_s \approx H_{ijk}$, its typical error is $\sim 20\%$. As far as it is possible to neglect the weak dependence of H_{ijk} on the plasma density ρ_s due to the presence of ρ_s in the Coulomb logarithm, the condition

$$q_{\text{in}} \geq q_{\text{ff}} + q_{\text{ec}} \quad (9)$$

defines a universal ignition boundary on the T_s, H_s plane (see curves *i* in Fig. 1). But, in contrast to the formation boundary *f*, the position of the ignition boundary *i* strongly differs for DT and D_2 fuels.

The ignition boundary for DT sparks shown in Fig. 1 has been calculated with only one fusion reaction, ${}^3\text{H}(\text{d}, \text{n}){}^4\text{He}$, and only alpha particle heating has been taken into account. It can be found easily that inequality (9) defines the minimum size, $H_s \geq 0.2 \text{ g}/\text{cm}^2$, for a DT spark. A more thorough analysis reveals, however, that condition (9) does not allow for the following additional possibility of spark ignition. Suppose that a narrow hot spark with the parameters T_s, H_s below curve *i* in Fig. 1 has been created. It will then cool down and spread over a broader plasma region owing to the electron thermal conductivity. If we assume further that such a spark decays, conserving its initial energy ($\rho_s T_s R_s^3 = \text{constant}$) and being under a constant pressure ($\rho_s T_s = \text{constant}$), the product $T_s H_s$ should be also conserved. In this case, a spark evolving in this way may eventually cross the high temperature branch of the ignition boundary *i* in the T_s, H_s parametric plane and ignite. This means that, along its high temperature branch, inequality (9) must be replaced by a weaker condition:

$$T_s H_s \geq \langle \text{TH} \rangle_0 \quad (10)$$

According to Eq. (9), in DT fuel, $\langle \text{TH} \rangle_0 \approx 1.5 \text{ g} \cdot \text{cm}^{-2} \cdot \text{keV}$. In Fig. 1, branch (10) is represented by line *e*. Note, however, that the two conditions $\rho_s T_s = \text{constant}$ and $\rho_s T_s R_s^3 = \text{constant}$ are not quite accurate for DT sparks with parameters in the vicinity of those characterizing line *e* (because $t_{\text{ec}} < t_s$ on the right hand side of curve *f*, and because thermonuclear heating together with radiative cooling also contribute to the energy balance), and criterion (10) turns out to be rather crude (for more details see below). In any case, as can be seen from Fig. 1, the modification of condition (9) with inequality (10) adds very little to the allowed region (hatched region) between the *f* and *i* curves where the spark ignition in DT fuel can occur.

In pure deuterium, thermonuclear heating of the spark must be calculated by properly taking into account the slowing down of a number of fast fusion products. We evaluate q_{in} under the assumption that tritium, which is born in the ${}^2\text{H}(\text{d}, \text{p}){}^3\text{H}$ reaction and is consumed in the much faster ${}^3\text{H}(\text{d}, \text{n}){}^4\text{He}$ reaction, is present from the very beginning in the equilibrium concentration, while the quantity of ${}^3\text{He}$ is negligibly small. Assuming further that the ${}^2\text{H}(\text{d}, \text{p}){}^3\text{H}$ and ${}^2\text{H}(\text{d}, \text{n}){}^3\text{He}$ reactions proceed with the same speed $\langle \sigma v \rangle_{\text{DD}}$, we obtain from Eq. (7)

$$\begin{aligned} q_{\text{in}} [\text{erg} \cdot \text{s}^{-1} \cdot \text{electron}^{-1}] &= 1.6 \times 10^{-6} \times \frac{1}{2} n_c \langle \sigma v \rangle_{\text{DD}} \\ &\times [0.82 + 2.45 f_{n2} + 3.02 f_p \\ &+ f_t (1.01 + 3.52 f_\alpha + 14.07 f_{n14} f_{\text{dr}})] \end{aligned} \quad (11)$$

Here the energy absorption coefficients f_p (for 3 MeV protons), f_t (for 1 MeV tritium nuclei) and f_α (for 3.5 MeV alpha particles) were calculated with Eq. (8); the absorption coefficients f_{n2} and f_{n14} for 2.45 MeV and 14 MeV neutrons were evaluated with Eq. (12) (see Section 3.1), with H_f being replaced by H_s . The absorption coefficient f_{dr} for the recoil deuterons with a mean energy of ~ 6 MeV was also calculated with Eq. (8), in which a double path length for the 3 MeV protons was used instead of the single path length for 6 MeV deuterons. Plasma heating by 0.82 MeV ${}^3\text{He}$ nuclei, whose range is $\leq 0.15 \text{ g}/\text{cm}^2$, was treated locally.

The resulting ignition boundary *i-e* for D_2 , as computed by Eqs (9)–(11), is also shown in Fig. 1. In contrast to the case of equimolar DT, the two allowed regions on the T_s, H_s plane, defined separately by the formation criterion and the ignition criterion, do not overlap. In other words, simple estimates of Eq. (5) and Eqs (9)–(11) indicate that spark ignition of pure D_2 fuel is not possible.

In conclusion, note that the above analysis is valid only for sparks created in the process of purely hydrodynamic implosion, when no external forces and heat sources act on the plasma and when no strong magnetic fields, which could significantly affect the electron thermal conductivity and the radiation losses, are present in the spark region.

3. RESULTS OF NUMERICAL CALCULATIONS

Numerical simulations of the spark ignition and the burn performance of DT and D₂ microspheres have been carried out with the 1-D hydrodynamics code DEIRA, starting from a compressed initial configuration with given spark parameters T_s, H_s and R_s. Step-like initial temperature and density profiles have been assumed, with the pressure being constant over the whole target. The implosion and spark formation stages are not discussed in this paper.

Two different target configurations have been investigated: (i) a bare fuel microsphere of mass M_f and (ii) a fuel microsphere of mass M_f tamped with a gold shell of mass M_t = 10 M_f. For equimolar DT, calculations have been performed with M_f = 1 mg and with a cold fuel temperature T_c of 0.5 keV. For D₂, the values M_f = 10 mg and T_c = 1 keV have been chosen. The above values of T_c represent reasonable lower limits to the compressed fuel temperature, as indicated by 1-D implosion simulations with realistic driving (laser or particle) pulse parameters. The initial temperature in the gold tamper was set at T_t = 0.1 keV and T_t = 0.3 keV for the DT and the D₂ targets, respectively; these values are low enough to have no effect on the equation of state for the tamper in its initial configuration.

3.1. Main features of the DEIRA program

The program DEIRA solves the equations of 1-D three-temperature hydrodynamics, similar to those presented in Ref. [2], by a Lagrangian method with the tensor artificial viscosity. In the equation of state and in the values of the transport and relaxation coefficients, the effects of Fermi degeneracy and of multiple ionization in high-Z materials are taken into account. DEIRA includes the kinetics of four principal nuclear fusion reactions: ³H(d,n)⁴He, ²H(d,p)³H, ²H(d,n)³He and ³He(d,p)⁴He. Target heating by fast fusion products, ³He at 0.82 MeV and T at 1.01 MeV, is calculated in the local approximation; the latter is justified when the spark in pure deuterium is large enough, H_s ≥ 1 g/cm². On-flight fusion reactions with these fast products are

ignored. Non-local energy deposition by fast alpha particles and by 3 MeV and 14.7 MeV protons is calculated by solving three non-steady diffusion equations (coupled with the hydrodynamic equations) for the energy density of these three fast species, as proposed earlier in Ref. [15]. The two groups of alpha particles, with energies of 3.52 MeV and 3.67 MeV, are combined into one group.

The heating by fast neutrons is evaluated in DEIRA only for the central fuel sphere, 0 ≤ r ≤ R_f, in the framework of the following simple approximation. First, the fraction of the total neutron energy is estimated which is deposited within the sphere r ≤ R_f, when neutrons scatter off the fuel deuterons and tritons. Then, this neutron power fraction is uniformly distributed over the central fuel mass, and divided between the plasma ions and electrons in proportion to the corresponding components of the drag force experienced by the recoil ions, but in the limit of an infinitely small path length for the latter.

The power fraction per neutron, deposited by fast neutrons in the fuel sphere r ≤ R_f, is approximated by the simple formula

$$\frac{\langle \Delta E_n \rangle}{E_{n0}} = \frac{H_f}{H_f + \tau_0 H_n} \quad (12)$$

where

$$H_f = \int_0^{R_f} \rho dr$$

and H_n is the mean free path (in g/cm²) of neutrons at their birth energy E_{n0}; in our case, H_n = 2A g/cm² for E_{n0} = 14 MeV, and H_n = 0.65A g/cm² for E_{n0} = 2.45 MeV; the neutron-fuel interaction is assumed to be dominated by elastic scattering. The parameter τ₀ can be evaluated in the limit H_f ≪ H_n, when it is sufficient to allow for one scatter only. We take β as the mean energy fraction lost by a neutron when it scatters off a nucleus with an atomic mass number A. Then, for three different neutron source distributions, we have

$$\tau_0 = \begin{cases} \beta^{-1} & \text{(source in the centre)} \\ \frac{4}{3} \beta^{-1} & \text{(uniformly distributed source)} \\ 2 \beta^{-1} & \text{(source along the outer sphere boundary)} \end{cases} \quad (13)$$

In the case of isotropic (in the centre-of-mass reference frame) elastic scattering, β is given by

$$\beta = \frac{2A}{(1+A)^2} = \begin{cases} \frac{4}{9} & A = 2 \\ \frac{3}{8} & A = 3 \end{cases} \quad (14)$$

However, as soon as we take into account that forward scattering is somewhat more probable than backward scattering, we arrive at the value $\beta \approx 1/3$, regardless of the tritium abundance. Finally, the value of $\tau_0 = \frac{4}{3} \beta^{-1} = 4$ has been adopted in DEIRA.

The error introduced by the assumption of uniform (over the fuel mass) neutron heating is not very large when either the ignition is uniform or the optical depth with respect to neutron scattering is not too large, $H_f \lesssim 1-3 H_n$. In cases where neither of these conditions is satisfied, this error can be checked by performing calculations in the local neutron heating approximation. Since we have neglected the finite path length of the recoil nuclei, we generally overestimate the neutron heating of the fuel. The error that we introduce in this way has a noticeable effect on the dynamics of targets with $H_f \approx 3-10 \text{ g/cm}^2$ when they enter the stage of strong thermonuclear burning ($T_{e,i} \geq 30 \text{ keV}$). Under such conditions, the neutrons lose a substantial fraction of their energy in the fuel region, but much of this energy is carried away by the recoil nuclei beyond the fuel sphere. An overestimated neutron heating leads to overestimated ion temperatures and, consequently, to underestimated values of the confinement time and of the fusion reaction rate (when $T_i \geq 100 \text{ keV}$). After performing check runs with an approximate treatment of the escape of recoil nuclei, we found that, in the most unfavourable cases, DEIRA may underestimate the target energy gains by approximately 10%.

For a comparison of DEIRA with other ICF codes, we have calculated the performance of the following two configurations with bare DT spheres: *Target 1* is a uniformly compressed DT microsphere with an initial density of 2000 g/cm^3 , an initial radius of $23.4 \mu\text{m}$ and an initial temperature of 5 keV . The thermonuclear yield calculated with DEIRA for this target is 11.69 MJ (Refs [1, 16, 12] give values of 10.49 MJ , 12.2 MJ and 11.12 MJ). *Target 2* has a uniform initial density of 6000 g/cm^3 , an initial radius of $7.36 \mu\text{m}$, and an initial temperature of 20 keV in the inner 10% of the volume and 1 keV in the outer cold region. The thermonuclear yield obtained with DEIRA for this target is 1.085 MJ (values of 1.245 MJ , 1.244 MJ and 1.12 MJ are given in Refs [2, 16, 12]).

3.2. Results for bare DT microspheres

In a number of publications the thermonuclear burn performance of compressed bare DT microspheres has

been calculated in the framework of the volume ignition scheme and in the framework of the spark ignition scheme [1, 2, 4, 12, 16]. None of these studies, however, gives a comprehensive answer to the question of by what factor spark ignition is energetically more efficient than uniform ignition. For example, the results presented in Refs [1, 2] may be incorrectly interpreted as indicating that spark ignition results in a fivefold increase of the energy gain compared with that of uniform ignition. Besides, almost all published calculations have been carried out for isochoric sparks, while an isobaric configuration seems to be much more realistic; in Ref. [6] it is reported that significantly lower limiting gains have been obtained. We make here an attempt to clear this issue.

The burn performance of compressed DT and D_2 microspheres is characterized by the energy gain, which is defined as the ratio of the total liberated thermonuclear energy to the initial energy of the compressed configuration. The volume ignition energy gain G_v and the spark ignition energy gain G_s are discussed separately.

3.2.1. Volume ignition

For a fixed fuel mass M_f the thermonuclear yield and the energy gain G_v depend on two parameters — the initial density ρ_f and the initial temperature T_f . The initial density can be expressed in terms of the confinement parameter $H_f = \rho_f R_f$:

$$\rho_f = 64.72 \text{ g/cm}^3 [H_f(\text{g/cm}^2)]^{3/2} [M_f(\text{mg})]^{-1/2} \quad (15)$$

Optimization of the gain $G_v(T_f, H_f)$ over two parameters was carried out in two steps. First, for a fixed value of H_f , the maximum with respect to T_f was sought:

$$G_{v_{m1}}(H_f) = \max \{G_v(T_f, H_f)\}_{|H_f = \text{constant}} \quad (16)$$

and then the absolute maximum was determined:

$$G_{v_m} = \max \{G_{v_{m1}}(H_f)\} \quad (17)$$

For $M_f = 1 \text{ mg}$, the largest volume ignition gain $G_{v_m} = 792$ occurs at $T_f = 1.1 \text{ keV}$ and $H_f = 22 \text{ g/cm}^2$ ($\rho_f \approx 6700 \text{ g/cm}^3$). Figure 2 illustrates the dependence of the intermediate maximum gain $G_{v_{m1}}$ (curve 1) and of the initial temperature $T_{f_{m1}}$ at which it occurs (curve 2) on the confinement parameter H_f . For $H_f < 22 \text{ g/cm}^2$, the gain $G_{v_{m1}}$ increases with increasing H_f because the optimum initial temperature $T_{f_{m1}}$ decreases owing to

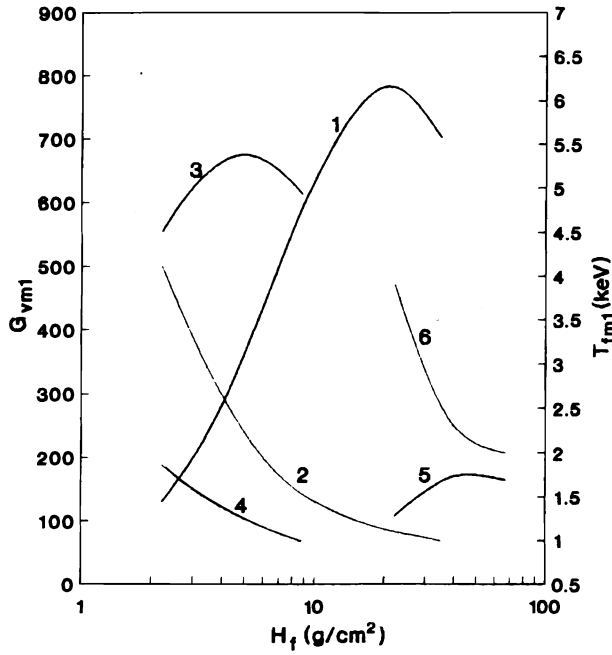


FIG. 2. Optimal parameters for volume ignition versus the fuel confinement parameter $H_f = \rho_f R_f$. Curves 1, 3 and 5 represent the energy gains of bare DT, tamped DT and tamped D_2 microspheres, respectively; curves 2, 4 and 6 show the optimal initial fuel temperatures for these cases.

the increasing fuel opacity for the bremsstrahlung radiation. Thus, our calculations clearly indicate that in uniformly ignited bare DT microspheres, it is possible to achieve sufficiently high energy gains, $G_v \approx 600\text{--}700$; however, for such gains, very high compressions are required, up to $H_f \geq 10 \text{ g/cm}^2$, which for $M_f = 1 \text{ mg}$ correspond to fuel densities ρ_f of $\geq 2000 \text{ g/cm}^3$.

3.2.2. Spark ignition

For a fixed fuel mass M_f of 1 mg and a cold fuel temperature T_c of 0.5 keV, the spark ignition gain G_s is a function of three initial parameters — the spark size H_s , the spark temperature T_s and the cold fuel density ρ_c . By means of the uniform pressure condition, the overall confinement parameter can be expressed in terms of the above three parameters:

$$H_f = H_s + \rho_c(R_f - R_s) \tag{18}$$

The optimization of G_s was conducted through the following steps:

$$G_{sm1}(H_s, \rho_c) = \max \{G_s(T_s, H_s, \rho_c)\}_{\substack{H_s = \text{constant} \\ \rho_c = \text{constant}}} \tag{19}$$

$$G_{sm}(H_s) = \max \{G_{sm1}(H_s, \rho_c)\}_{H_s = \text{constant}} \tag{20}$$

Numerical calculations showed that the second maximum $G_{sm}(H_s)$ is a very weak function of H_s (when H_s was varied from 0.3 g/cm² to 0.1 g/cm², G_{sm} changed from 1425 to 1450), and we will ignore this dependence in the following discussion.

Table I lists the values of G_{sm1} , calculated for different values of ρ_c , together with the spark temperatures and the H_f values at which the maximum of G_{sm1} occurs. The value ρR of the spark was fixed at $H_s = 0.2 \text{ g/cm}^2$. This value corresponds approximately to the lower edge of the hatched region in Fig. 1. The highest spark ignition gain, $G_{sm} = 1444$, is reached at $H_f \approx 6 \text{ g/cm}^2$. This optimum value of H_f is practically independent of H_s and agrees with the value obtained in Ref. [12] for spark configurations with uniform density. Our value of G_{sm} is also close to that reported in Ref. [12] when it is renormalized to the cold fuel temperature T_c of 1 keV and when we allow for an error of $\sim 10\%$ in the initial target energy introduced in Ref. [12] by a simplified treatment of the Fermi degeneracy.

TABLE I. OPTIMAL PARAMETERS OF BARE SPARK IGNITED DT MICROSPHERES

ρ_c (g/cm ³)	300	424	600	848	1200	1697	2400
T_{sm1} (keV)	9.3	8.5	7.4	8.0	8.6	9.3	10.0
H_f (g/cm ²)	0.67	1.3	2.3	3.4	4.7	6.6	9.0
G_{sm1}	30	237	976	1300	1417	1444	1429

In Table I, it can be seen that the optimum spark temperature T_{sm1} is rather insensitive to the compressed fuel density ρ_c . However, the results discussed in Section 2 imply that T_{sm1} should strongly depend on H_s when $H_s < 0.3 \text{ g/cm}^2$. From numerical results, we have deduced the following approximate relationship:

$$H_s \cdot T_{sm1}^{3/2} \approx \text{constant} \approx 5 \text{ g} \cdot \text{cm}^{-2} \cdot \text{keV}^{3/2} \tag{21}$$

At the same time, the values of the threshold spark ignition temperature $T_{si} = T_{si}(H_s)$, marked by crosses in Fig. 1, in bare DT spheres fall considerably below the optimum values T_{sm1} .

3.2.3. Spark factor

Having compared the optimum spark ignition configuration with the optimum volume ignition configuration, we arrive at the following value of the spark factor for a bare 1 mg DT microsphere:

$$f_s \equiv \frac{G_{sm}}{G_{vm}} = 1.82 \quad (22)$$

The unexpectedly low value of f_s is due to the rather large volume ignition gains G_v . However, to reach a maximum value of G_v , a very high compression of the fuel is needed, i.e. $H_f \approx 20 \text{ g/cm}^2$ (see Fig. 2); this does not seem to be realistic. To account for possible constraints on the maximum fuel density, we introduce a differential spark factor:

$$f_{sp} = \frac{G_{sm1}(H_s, \rho)}{G_{vm1}(\rho)} \quad (23)$$

which is defined as the ratio of maximum gains, with the restriction that the fuel density does not exceed some fixed value of ρ (provided that $\rho \leq 2000 \text{ g/cm}^3$). Comparing the results presented in Table I and in Fig. 2, we find that the differential spark factor has a maximum of $f_{sp} \approx 3.2$ at $\rho \approx 850 \text{ g/cm}^3$.

The spark factor would be expected to increase with increasing DT fuel mass M_f because, for higher values of M_f , less specific energy input is required to compress the mostly cold fuel to the same value of H_f , whereas for volume ignition the specific energy input cannot be reduced below $\sim 1.5 \text{ keV}$ per particle. It is easy to verify that, asymptotically, for very high values of M_f , the spark factor should grow as $f_s \propto M_f^{1/3}$. Our calculations indicate, however, that for a few milligrams of equimolar DT, almost no growth of f_s with M_f is observed: for $M_f = 4 \text{ mg}$ we found the same value ($f_s = 1.8$).

3.3. Results for tamped DT microspheres

In all realistic target designs, thermonuclear fuel is surrounded by some non-fuel material. In the course of the implosion process, some of this inert material will be also compressed, forming a high density tamper around the fuel. We assume that, initially, at maximum compression, the tamper and the fuel have equal pressures. The energy gain of a tamped fuel microsphere is defined as the ratio of the total liberated thermonuclear energy to the *sum of the energies of the initially compressed fuel and the tamper*.

When a massive tamper with $M_t \gg M_f$ is added, it affects the target energy gain in two different ways. On the one hand, more energy is needed to compress a target with the same fuel mass; on the other hand, the confinement time becomes longer for the same H_f values and more fuel is burned. As was shown by Mason and Morse [17], these two effects approximately cancel each other as long as $M_t \leq 10 M_f$. However, the question of how the introduction of a massive tamper affects the values of the spark factor f_s does not seem to have been discussed in the literature so far.

3.3.1. Volume ignition

With fixed fuel ($M_f = 1 \text{ mg}$) and tamper ($M_t = 10 \text{ mg}$) masses, the gain coefficient $G_v(T_f, H_f)$ was optimized in the same way as for bare DT spheres (see Eqs (16) and (17)). A plot of $G_{vm1}(H_f)$ is shown in Fig. 2 (curve 3). It can be seen that, in contrast to bare DT spheres, the optimum gain G_{vm1} depends only weakly on the fuel H_f values over the range $2 \text{ g/cm}^2 \leq H_f \leq 10 \text{ g/cm}^2$. The maximum volume ignition gain $G_{vm} = 677$ occurs at $H_f \approx 4.5 \text{ g/cm}^2$ ($\rho_f \approx 600 \text{ g/cm}^3$), which is much lower than the optimum compression of bare DT spheres. This can be explained by the fact that, in addition to the longer confinement time achieved in this case, a massive tamper provides an effective screen for the fuel bremsstrahlung radiation. As a result, the optimum ignition temperature $T_{fm1}(H_f)$ is almost a factor of two lower than that for bare DT spheres (see curves 4 and 2 in Fig. 2). Thus, when a tamped 1 mg DT sphere is compressed to a value $H_f \approx 3 \text{ g/cm}^2$ ($\rho_f \approx 300 \text{ g/cm}^3$), which is certainly not an extreme value, sufficiently high volume ignition energy gains, $G_v \approx 600$, can be achieved.

3.3.2. Spark ignition

Similar to the target gain in the case of bare DT spheres, the target gain $G_{sm}(H_s)$ optimized with respect

TABLE II. OPTIMAL PARAMETERS OF TAMPED SPARK IGNITED DT MICROSPHERES

$\rho_c \text{ (g/cm}^3\text{)}$	300	424	600	848
$T_{sm1} \text{ (keV)}$	6.3	6.3	6.8	6.8
$H_f \text{ (g/cm}^2\text{)}$	1.1	1.7	2.5	3.7
G_{sm1}	1095	1250	1270	1190

to the spark temperature T_s and the cold fuel density ρ_c (see Eqs (19) and (20)) depends only weakly on H_s : when H_s decreases from 0.3 g/cm^2 to 0.1 g/cm^2 , G_{sm} increases from 1190 to 1310. Table II shows the optimal gains $G_{sm1}(H_s, \rho_c)$ as calculated for $H_s = 0.2 \text{ g/cm}^2$ and various ρ_c values, together with the optimal spark temperatures T_{sm1} and the fuel confinement parameters H_f (see Eq. (18)). The optimum spark temperature T_{sm1} is determined by the spark size H_s ; T_{sm1} falls close to the ignition threshold, whose position can be approximated by

$$H_s \cdot T_{si}^{3/2} \approx 3.5 \text{ g} \cdot \text{cm}^{-2} \cdot \text{keV}^{3/2} \quad (24)$$

In Fig. 1, a few points along the ignition boundary as calculated by DEIRA for tamped DT spheres are indicated by squares.

It should be noted that the above threshold parameters for spark ignition are close to those obtained in Ref. [18] if detonation is neglected. The physical reason for this is obvious. A spark configuration at uniform pressure can initiate a propagating burn wave by means of either the electron heat conduction or the energy transport by fast fusion products, but not by emanation of a strong shock wave; rather, a detonation wave should be typical for isochoric sparks. More precisely, a comparison of our results with those obtained in Ref. [18] reveals that for the same temperatures T_s , isobaric sparks ignite at much lower H_s values (by a factor of two to five) than do the isochoric sparks.

The spark factor for the tamped 1 mg DT spheres, $f_s = 1.88$, is practically equal to the value for the bare fuel configurations. A major difference with regard to the case of a bare sphere arises, however, when an upper bound on the possible fuel densities is imposed; in this case the differential spark factor f_{sp} defined in Eq. (23) preserves its value ($f_{sp} = 1.8-1.9$) over a wide range of initial fuel densities, $300 \text{ g/cm}^3 \leq \rho_f \leq 1000 \text{ g/cm}^3$.

3.4. Results for tamped D_2 microspheres

As was demonstrated by the time-scale analysis in Section 2, spark ignition of D_2 microspheres is not possible because a hot and sufficiently large fuel region cannot be created in the process of hydrodynamic implosion. Nonetheless, to examine this problem more closely, we have performed the same set of calculations as for the 1 mg DT sphere also for a 10 mg D_2 microsphere tamped with a 100 mg gold shell, with the assumption that a spark with the necessary parameters already exists, skipping the problem of its formation.

3.4.1. Volume ignition

The temperature optimized gain $G_{vm1}(H_f)$ is shown in Fig. 2, curve 5. It reaches a maximum of $G_{vm} = 176$ at $H_f = 42 \text{ g/cm}^2$ ($\rho_f \approx 5600 \text{ g/cm}^3$) and $T_f = 2.2 \text{ keV}$.

3.4.2. Spark ignition

When the target gain was optimized over T_s and ρ_c according to Eqs (19) and (20), it was found that the maximum gain, $G_{sm}(H_s) = 204$, does not depend on H_s (at least in the range $1 \text{ g/cm}^2 \leq H_s \leq 10 \text{ g/cm}^2$). This maximum occurs at $\rho_c \approx 8000 \text{ g/cm}^3$ and $H_f \approx 33 \text{ g/cm}^2$; this optimum value of H_f is also almost independent of H_s . On the contrary, the optimum spark temperature T_{sm1} is determined by the value of H_s and obeys the relationship

$$H_s \cdot T_{sm1} \approx 50 \text{ g} \cdot \text{cm}^{-2} \cdot \text{keV} \quad (25)$$

One can easily verify that the straight line given by Eq. (25) on the $(\log T_s, \log H_s)$ plane passes considerably below the ignition boundary i-e for the D_2 fuel (see Fig. 1). Thus, even if we assume that the formation process puts no constraint on the possible D_2 spark parameters, the optimum values of these parameters for a 10 mg microsphere are in the region where no spark ignition in the proper sense of the word can occur. In this case, one would expect the spark factor to be exactly unity. The slightly larger value, $f_s = 204/176 = 1.16$, can be explained by a non-linear temperature dependence of the thermonuclear reaction rates, making a non-uniform temperature distribution more advantageous than a uniform one with the same total energy [2].

Note that the approximate procedure for evaluating neutron heating, described in Section 3.1 and based on distributing the deposited neutron energy uniformly over the entire fuel, considerably underestimates the heating of relatively large sparks (with $H_s \geq 1-3 \text{ g/cm}^2$) in D_2 fuel by 2.45 MeV neutrons. To check for possible errors, the performance of D_2 microspheres was recalculated, with the approximation of local heating by 2.45 MeV neutrons. As a result, the maximum gain somewhat increased to 212, while the other parameters of the optimum configuration remained unchanged.

4. DISCUSSION AND BASIC CONCLUSIONS

In contrast to previous investigations of the burn performance of precompressed thermonuclear fuel, we

have explored the relative effectiveness of spark ignition in DT and D₂ microspheres surrounded by a massive high-Z tamper. Apart from the fact that tamped fuel spheres are more realistic, they have the important advantage over the bare configurations that a considerably lower fuel compression (by a factor of five to ten in fuel density) is required to produce almost the same maximum energy gains. It is shown that, irrespective of possible constraints on the maximum fuel density, a hot spark in the centre of DT fuel of a few milligrams can provide no more than a twofold increase in the optimum volume ignition energy gain. In D₂ targets, this increase does not exceed 15–20%.

To obtain gain coefficients of the whole-set targets, the above G_v and G_s values, calculated for *tamped* DT (or D₂) microspheres, have to be multiplied by the hydrodynamic efficiency η . The hydrodynamic efficiency is largely determined by specific target driver coupling physics and can be calculated separately from the burn phase. As demonstrated in Ref. [19], in hollow spherical targets illuminated by heavy ion beams, η values of ≈ 0.2 – 0.25 can be achieved. Combining this result with the above values of G_{vm} , we conclude that targets driven by heavy ion beams, with a uniform ignition of ≈ 1 mg of DT fuel, can produce large energy gains, $G_{max} \approx 130$ – 170 ; to achieve this, the DT fuel must be compressed to $H_f \geq 3$ g/cm² ($\rho_f \geq 300$ g/cm³). For D₂ targets with $M_f \approx 10$ mg, an analogous estimate leads to $G_{max} \approx 30$ – 40 for $H_f \geq 30$ g/cm² ($\rho_f \geq 3000$ g/cm³).

It should be noted, however, that these conclusions have been obtained from the idealistic one-dimensional treatment, with no regard being paid to hydrodynamic instabilities at the fuel–tamper interface. With a density contrast of approximately a factor of ten, such instabilities during the deceleration and stagnation phases of the implosion (even if they are alleviated by adopting a more sophisticated target design) are likely to degrade the performance of tamped DT and D₂ microspheres. As a result, the maximum gains achievable in realistic targets are likely to be lower and to require higher H_f and T_f values than those mentioned above. However, since it is not clear which of the two ignition schemes will suffer more from hydrodynamic instabilities, it is possible that the values of the spark factor f_s may be the same as those reported above, even when these instabilities are properly taken into account.

Our calculations indicate that the widely used approximate formula

$$f_b = \frac{H_f}{H_f + H_b} \quad (26)$$

for the fractional burnup in bare DT spheres is very inaccurate: to account for the variation of f_b along curve 1 in Fig. 2, the value of H_b has to be changed from ≈ 9 g/cm² at $H_f = 3$ g/cm² to ≈ 24 g/cm² at $H_f = 22$ g/cm². The suggestion of Mason and Morse [17] that the fractional burnup in tamped DT spheres depends on the total confinement parameter $H = H_f + H_t$ in the same way as it depends on H_f in bare DT spheres was not confirmed; for the target with $H_f = 8.8$ g/cm² along curve 1 in Fig. 2 we obtained $f_b = 0.33$, while for the target with $H_f + H_t = 8.8$ g/cm² along curve 3 in Fig. 2 we obtained $f_b = 0.53$.

Meyer-ter-Vehn [6] found that the limiting gains of spark ignited bare DT spheres with isobaric initial conditions fall considerably below those obtained in Ref. [3] for isochoric sparks (by a factor of three to five). On the contrary, our results, when renormalized to the same initial conditions and compared with those reported in Ref. [12], exhibit close agreement between the isochoric and the isobaric limiting spark ignition energy gains. This discrepancy may be due partly to the not very accurate approximations (similar to Eq. (26)) used in the simple models of Refs [3, 6] and partly to the fact that no optimization over the spark parameters was carried out in the previous studies.

ACKNOWLEDGEMENTS

The author would like to acknowledge helpful discussions with V.S. Imshennik, P.V. Sasorov and M.D. Churazov.

REFERENCES

- [1] BRUECKNER, K.A., JORNA, S., *Rev. Mod. Phys.* **46** (1974) 325.
- [2] FRALEY, G.S., LINNEBUR, E.J., MASON, R.J., MORSE, R.L., *Phys. Fluids* **17** (1974) 474.
- [3] KIDDER, R.E., *Nucl. Fusion* **16** (1976) 405.
- [4] KIDDER, R.E., *Nucl. Fusion* **19** (1979) 223.
- [5] BODNER, S.E., *J. Fusion Energy* **1** (1981) 221.
- [6] MEYER-TER-VEHN, J., *Nucl. Fusion* **22** (1982) 561.
- [7] METZLER, N., MEYER-TER-VEHN, J., *Laser Part. Beams* **2** (1984) 27.
- [8] TAHIR, N.A., LONG, K.A., *Nucl. Fusion* **23** (1983) 887.
- [9] TAHIR, N.A., LONG, K.A., *J. Phys. (Les Ulis)* **49** (1988) C7–193.
- [10] VELARDE, G., ARAGONES, J.M., GAGO, J.A., et al., *Laser Part. Beams* **4** (1986) 349.
- [11] CICCHITELLI, L., ELIEZER, S., GOLDSWORTHY, M.P., et al., *Laser Part. Beams* **6** (1988) 163.
- [12] HARRIS, D.B., MILEY, G.H., *Nucl. Fusion* **28** (1988) 25.
- [13] SPITZER, L., *Physics of Fully Ionized Gases*, Interscience Publ., London (1956).

BASKO

- [14] KROKHIN, O.N., ROZANOV, V.B., *Kvantovaya Elektron.* **4** (1972) 118.
- [15] BASKO, M.M., *Fiz. Plazmy* **13** (1987) 967; *Sov. J. Plasma Phys.* **13** (1987) 558.
- [16] JARVIS, O.N., *J. Phys.*, **G 2** (1976) 603.
- [17] MASON, R.J., MORSE, R.L., *Nucl. Fusion* **15** (1975) 935.
- [18] AVRORIN, E.N., FEOKTISTOV, L.P., SHIBARSHOV, L.I., *Fiz. Plazmy* **6** (1980) 965; *Sov. J. Plasma Phys.* **6** (1980) 527.
- [19] BASKO, M.M., *Laser Part. Beams* **8** (1990) 409.

(Manuscript received 2 April 1990

Final manuscript received 16 July 1990)